PULSED SEXTUPOLE INJECTION FOR BAPS *

Y. Jiao#, G. Xu, IHEP, Beijing 100049, China

Abstract

In this paper we present the physical design of the pulsed sextupole injection system for Beijing Advanced Photon Source (BAPS) with an ultralow emittance. The BAPS ring lattice is designed in such a way that two injection options are allowed, i.e., with septum and pulsed sextupole in different drift spaces or in the same drift space. For both options optimal conditions are obtained for high injection efficiency. It is found that the available efficiency in a storage ring with limited acceptance can be affected by position-dependent dispersive effect induced by the pulsed sextupoles.

INTRODUCTION

"Ultimate" storage rings (USRs) [1], with equal transverse emittances at diffraction limit for X-rays of interest for user community and with much higher performance than existing rings, have been extensively studied in the past few years. It is believed that USRs can provide highly stable photon beams having low peak brightness with high average brightness and high pulse repetition rate, photons that do not over-excite or damage samples the way those from free electron lasers do, and they can serve a large number of diverse users simultaneously. However, associated with reduced emittance and demanding lattices, several technical challenges exist for the actual implementation of USRs, one of which is to inject the electron beam into the storage ring with high efficiency. The proposed methods include on-axis "swap-out" injection [2] and off-axis injection with pulsed multipole magnets [3-4]. The application of the latter scheme, i.e., injection with a pulsed sextupole, on the Beijing Advanced Photon Source (BAPS) is thoroughly discussed in this paper.

The principle of the pulsed sextupole injection is rather simple [4]. The injected bunch from the transfer line is deflected into the ring by a septum magnet. After passing a section of the beam line of the ring, it enters the pulsed sextupole at (x, x'), with $0 < |x| < min(x_{ph}, x_{dy})$, where x_{ph} and x_{dy} are the horizontal physical and dynamic aperture, respectively. Once the normalized integral sextupole field strength $K_2 = B''l/(B\rho)$ satisfies

$$x' + \frac{1}{2} K_2 x^2 = 0, \qquad (1)$$

the injected beam will be captured into the ring, where B'' and l are the sextupole gradient and length, respectively; $(B\rho)$ is the magnetic rigidity of the reference particle. By contrast, the stored beam passing the pulsed sextupole through the magnetic center sees approximately zero kick, and thus experiences little disturbance.

*Work supported by the special fund of the Chinese Academy of Sciences under contract No. H9293110TA.

#jiaoyi@ihep.ac.cn

BAPS, a 5-GeV storage ring-based light source, is planned to be built in Beijing to satisfy the increasing scientific requirements from user community. A storage ring with circumference of 1364.8 m and natural emittance of 51 pm is recently designed. The emittance can be further decreased to diffraction limit level (~10 pm) in both transverse planes with damping wigglers and locally-round beam production method [5]. The lattice layout and the optical functions along the ring are presented in Fig. 1. Except 34 standard low-beta sections for high-brightness radiation, there are two high-beta injection sections. To restore the periodicity, the phase advance of injection section is tuned to be that of standard section adding 0 or 2π, which, together with high-beta function design, results in large horizontal dynamic aperture x_{dy} (> 10 mm) that promises injection at a relative large x, although with a price of relatively small acceptance of the horizontal angular deviation (on the scale of 0.1 mrad, see Fig. 2). Since there are ample drift spaces in the injection section, two injection options are promised. As shown in Fig. 3, the septum magnet and the pulsed sextupole can be placed in different drift spaces, or in the same drift space. The quadrupole between the septum and the pulsed sextupole results in larger phase advance between IP and PSM, smaller sextupole strength and higher injection efficiency in the first option. However, for the same reason the first option is mode-dependent, i.e., the optimal solution for injection needs to vary with the change of the ring optics. Since the optimization processes for the two options are similar, we will present the detailed analysis for the first option, while show only the main results for the second.

The injected beam is presumed to be extracted from a 400-m booster, with emittance ε_x of 4 nm and rms energy spread σ_δ of 0.1%. In this paper, the end of the transfer line, i.e., the end of the septum magnet is referred to as the injection point (IP), and the end of the pulsed sextupole magnet is denoted as PSM.

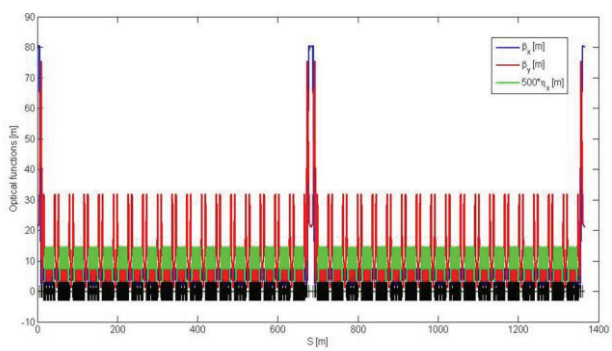

Figure 1: Lattice layout and the optical functions for one design of the BAPS storage ring.

ISBN 978-3-95450-122-9

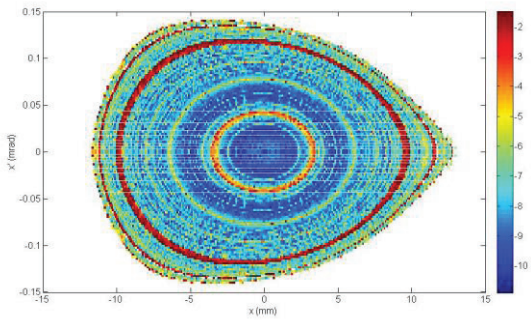

Figure 2: On-momentum horizontal acceptance in the middle of the injection section. The colours, from blue to red, represent the stabilities of the particle motion, from stable to unstable.

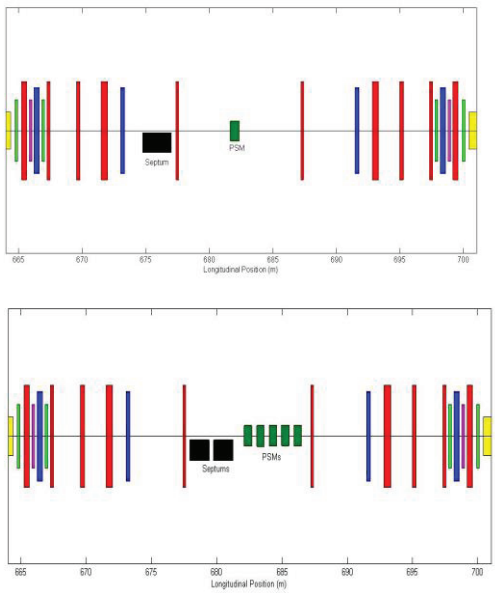

Figure 3: Two injection options, with septum and pulsed sextupole located in different drift spaces (upper plot) or in the same drift spaces (lower plot).

In the following, the injection system is first simplified by considering the injected beam as a "point" charge to calculate the magnetic parameters of the injection system and the optimal dispersion functions at the IP. Then the injection efficiency is optimized by considering finite-emittance beam, where the position-dependent dispersive effect [6] induced by pulsed sextupole is discussed.

INJECTION WITH A POINT CHARGE

In the first injection option, a 2-m septum magnet is located in a 4-m drift space, 0.5 m from the downstream closest quadrupole; the end of the 0.7-m pulsed sextupole is at the center of the next 9.6-m drift space (see Fig. 3). The position of the injected bunch relative to the stored beam at the IP is shown in Fig. 4. The blade is at -9 mm from the trajectory of the unperturbed stored beam, with a thickness of 2.5 mm. The injected bunch at the IP is at $x_{inj,c}$ = -14 mm, where the subscript "*c*" indicates the centre of the beam. In this section we consider only the central orbit of the injected bunch. In other words, the injected bunch is treated as a "point" charge.

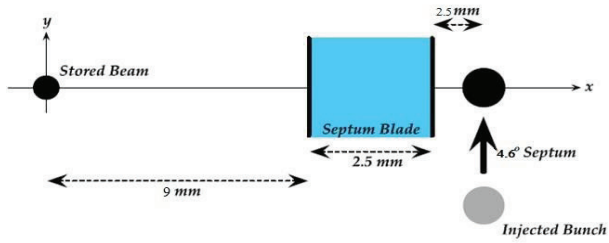

Figure 4: Schematic view of the position of the injected bunch relative to the stored beam at the IP.

The injected bunch starts from the IP with coordinate of $X_{IP,0} = (x_{IP,0}, x'_{IP,0}, \delta_{IP,0})^T$ = (-14 mm, $x'_{IP,0}$, 0) ^{T}, where the superscript "T" means the transpose of a vector (or a matrix), the subscript "0" indicates zero momentum deviation. The value of the $x'_{IP,0}$ is scanned to record the horizontal offset at the PSM, x_{psm}, with which the required K_2 is calculated. As a compromise of small K_2 and high tolerance of the magnetic errors, the solution with a moderate x_{psm} is chosen, x_{psm} = -5 mm, $x'_{IP,0}$ = -0.64 mard and K_2 =151.2 m^{-2}.

Besides, it is necessary to ensure the off-momentum particles can also be captured. Consider a bunch starting from the IP with coordinate of $X_{IP,\delta}$ = (-14 mm, -0.64 mrad, δ) ^{T},

$$X_{psm,\delta} = \mathcal{M}_{I2P} X_{IP,\delta}, \quad (2)$$

where $\mathcal{M}_{I2P}$ refers to the transfer map from IP to PSM.

Simulation shows that there exists dispersive effect from IP to PSM,

$$\begin{aligned} x_{psm,\delta} &= x_{psm,0} + A\delta, \\ x'_{psm,\delta} &= x'_{psm,0} + B\delta, \end{aligned} \quad (3)$$

with A = -0.012, B = -0.008. This effect will be corrected when the dispersion function (D_x, D_x') at the IP is set to (0.0088 m, 0.0017) so that (A, B) = (0, 0).

INJECTION WITH A REAL BEAM

Further study is done by considering a finite-emittance beam (ε_x = 4 nm). The injection efficiency is optimized as follows: a) generate beam distribution with pre-defined Courant-Snyder parameters (α_0, β_0) and with δ = 0 at PSM, denote it as distribution **A**; b) trace back to IP, record the beam distribution, denote it as distribution **B**, calculate corresponding (α, β) by statistics; c) re-generate beam distribution at IP with the obtained (α, β) and with σ_δ = 0.1%, denote it as distribution **C**; d) track particles from IP to PSM, record the final beam distribution and denote it as distribution **D**; e) track the particles for 6000 turns (~1 damping time) to calculate the survive rate, i.e., the injection efficiency.

The (α_0, β_0) are varied and the procedures a) to e) are repeated to search for the best optical condition. The variation of injection efficiency with the σ_x of distribution **A** is shown in Fig. 5. The maximum efficiency is 99.9%,

ISBN 978-3-95450-122-9

for which the capture processes are shown in Fig. 6. The optimal conditions for both options are listed in Table 1.

During optimization, we note that the dispersive effect induced by the pulsed sextupole has non-ignorable impact on the injection. Figure 7 shows the tracking results with the σ_x of distribution **A** equal to 0.3 mm. One can see that the distributions **C** and **D** are somewhat different from the distributions **B** and **A**, respectively, although the optimal dispersion condition obtained previously is already used. Study shows that this difference is caused by the pulsed sextupole. For the injected particles, the pulsed sextupole acts like a bending magnet whose kick varies with the offset of injected particle at PSM, resulting in position-dependent dispersion. The residual dispersion in term of the x_{psm} is shown in Fig. 8. Compared with the limited ring acceptance, the residual dispersion will cause a relatively large diffusion in the phase space, leading to difficulty in optimization of the injection efficiency. To reduce this unwanted effect, a small rms horizontal beam size of the injected beam at the PSM is preferred.

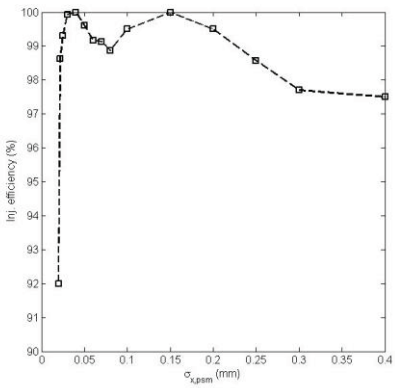

Figure 5: Variation of injection efficiency with the σ_x of distribution **A**.

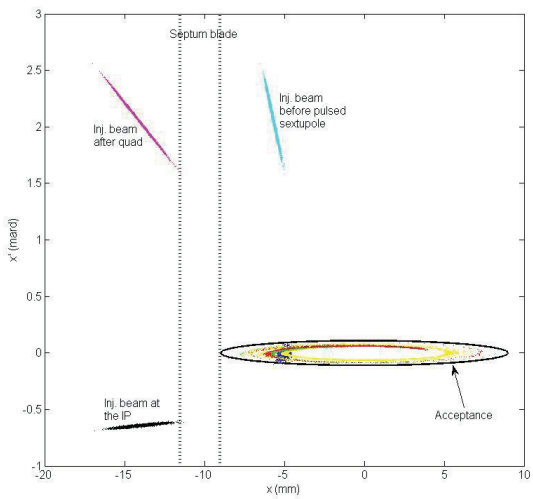

Figure 6: Numerical tracking data for the injection and the capture processes with the optimal conditions for the first injection option. The particles captured in the first three turns are in colours of blue, green, red, respectively. The particles captured at the 6000th turn are in yellow.

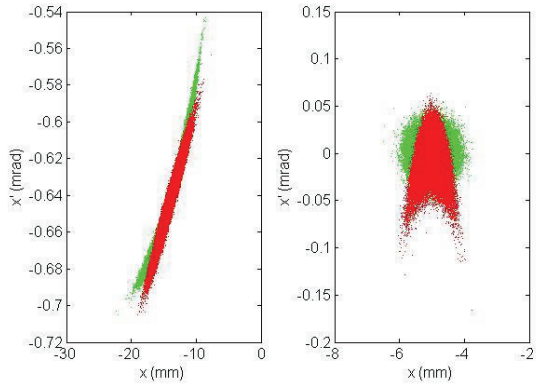

Figure 7: Simulation data of the distributions **A** (right plot, green), **B** (left plot, green), **C** (left plot, red) and **D** (right plot, red), with the σ_x of distribution **A** equal to 0.3 mm.

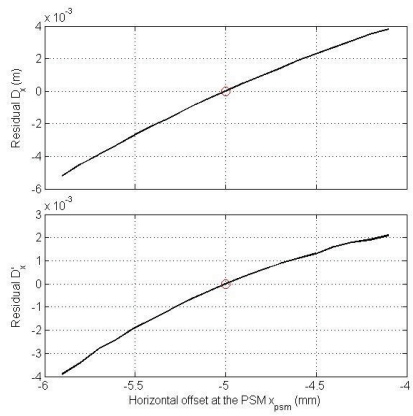

Figure 8: Residual dispersion functions in term of the x_{psm}. The circles indicate the case for the reference particle.

Table 1: Optimal Conditions for Two Injection Options

Parameters	1st option	2nd option
D_x at IP	0.0088 m	0.0332 m
D'_x at IP	0.0017	0.0074
β_x at IP	145.7 m	260.8 m
α_x at IP	2.0	96.5

REFERENCES

[1] M. Bei, *et al.*, Nucl. Instrum. Methods Phys. Res., Sect. A **622**, 518 (2010).
[2] M. Borland, Nucl. Instrum. Methods Phys. Res., Sect. A, **557**, 230 (2006).
[3] K. Harada, *et al.*, Phys. Rev. ST Accel. Beams **10**, 123501 (2007).
[4] H. Takaki, *et al.*, Phys. Rev. ST Accel. Beams **13**, 020705 (2010).
[5] G. Xu, *et al.*, Chin. Phys. C, **37**(6), 067002, (2013).
[6] S.C. Leemann, Phys. Rev. ST Accel. Beams **15**, 050705 (2012).